J Therm Anal Calorim (2011) 106:85–91
DOI 10.1007/s10973-010-1270-2

Methodology of interpreting thermal analysis of polymers

Bernhard Wunderlich

NATAS2010 Conference Special Issue

Abstract The goal of the thermal analysis experiments is to extract scientifically and technological important information from measurements of "heat." Unfortunately, there exists no direct heat meter. In fact, the assessment of the quantity heat has a colorful past and, as is a common human trait, the back-integration of successively gained knowledge into the basic teaching is lax, as in all stages of education. Thermal analysis can be taken as a prime example of this problem. A "Methodology of Interpreting Thermal Analysis of Polymers" is described in this report on the example of recent data on poly(butylene terephthalate), PBT, crystallized by slow cooling from the melt. It is shown how the simple temperature-difference or heat-flow rate as a function of sample temperature is converted to calorimetric information. Once calorimetric data are available, the results can be interpreted using modern descriptions of phases, making use of a scheme of phase structures as well as considering molecular motion arguments and phase sizes. Using the three classical types of strong chemical bonding leads to 57 possible condensed phases and two types of transitions (glass and order/disorder transitions) necessary for the description.

Keywords Methodology · Thermal analysis · Phase scheme · Order–disorder transitions

B. Wunderlich
Department of Chemistry, The University of Tennessee, Knoxville, TN 37996-1600, USA

B. Wunderlich (✉)
200 Baltusrol Road, Knoxville, TN 37934-3707, USA
e-mail: Wunderlich@CharterTN.net

Introduction

The goal of the interpretation of thermal analysis is to extract all scientifically and technological important information from measurements of "temperature" and "heat." The international system of units established in 1960, SI (Système International d'Unités), uses the "thermodynamic temperature, T" (in units of K) as one of its seven base units (For proper units see the continually updated information of the IUPAC, [1]). The Celsius temperature, °C (=$T - 273.15$), is thought to be more practical for daily use, but should be abolished as much as practical. A number of thermometers exist which can easily be calibrated in K (or °C) using the definitions, techniques, and standards [2, Sects. 4.1, 4.3.4, and Appendix 8].

Unfortunately, there exists no direct heat meter. In fact, the assessment of the quantity heat has a colorful past, and even today is often poorly understood [2, Sect. 2.1.1]. Have you not frequently heard the statement (and accepted it as being correct): "The heat in this room is unbearable." If so, you permit the common confusion of the term "heat" with "temperature." This could not be helped before the eighteenth century when the scientific understanding of "heat" was limited. Since then, "heat" is properly identified as a form of energy (in joule, J, in SI, base units: kg m^2 s^{-2}), characterized by its intensive parameter, "temperature." Thus, the proper statement is "The temperature in this room is unbearable."

It is a common human trait to be lax with the back-integration of new knowledge into the basic teaching [3]. Misconceptions in chemistry exist all throughout our system of education [4]. An old example is the late recognition of the digit "zero" for proper counting in Western Civilization. Only in the twelfth century was "zero" introduced as a digit *and* place-holder as the basis for the decimal

system (as in 0, 10, 100, etc.) [3, pp. 9-85-86]. This led to the 1 year early start of the twenty-first century and the mistaken belief by many, that today's NATAS Meeting is in the first year of the second decade of this century. If this and many other known improvements were taught in kindergarten, time and effort could be saved, even in graduate thermal analysis courses.

Interpretation of thermal analysis data

Let us see the methodology to be followed and pitfalls to be avoided on the example of the interpreting the thermal analysis of poly(butylene terephthalate), PBT. The chosen measurement was done recently on a PBT melt, crystallized by slow cooling [5]. The sample was fully described to the best of knowledge with molar mass, purity, etc., as is necessary to connect the new information gained to prior and later research and applications. Today's basic thermal analysis technique is differential scanning calorimetry, DSC, i.e., the time scale of the scanning is also a characteristic of the measurement. The data gained are to be expressed in units of heat (in joule, J), defined one hundred years ago, and internationally accepted for over 50 years [1] (since then, not to be given in calories anymore!).

Figure 1a illustrates the typical differential thermal analysis, DTA. It contains a plot of the sample temperature, T (in K), and its difference from the reference temperature, ΔT. There is no heat recorded, i.e., it cannot be considered "calorimetry," but, at a known rate of temperature change, the measured ΔT is proportional to the heat-flow rate (in J s^{-1} or W) at the measured T. From this description, it is clear that the precision depends critically on the construction of the instrument and its calibration [2]. The heat-flow rate and time can be computed from ΔT and T, respectively, by applying the proper calibrations.

While the curve in Fig. 1a is a DTA trace, the subsequent representations, b–f, are DSC traces. The curves of Fig. 1 are not "thermograms," since the thermogram is "the record by writing or printing involving the use of heat" [6], the heat, however, is the object of the measurement, not the writing tool. The basic trace represents the measurement of ΔT between the sample-filled container and a second, empty, but otherwise identical, reference container versus the sample temperature. Commonly, the containers are aluminum, gold, or platinum pans to conduct the heat quickly into the sample to be measured. Since researchers and manufacturers could not agree on how to plot the heat-flow direction in a DSC trace, one is required to indicate the exothermic or endothermic direction of the ordinate. Chemists considered heat flow into the sample as positive, while engineers considered heat flow into the sample as a loss from the heat available for the engineering interest, and thus count it as negative! Although one can see interesting thermal events from the DTA trace of Fig. 1a, it is far from giving quantitatively interpretable calorimetric results, only the temperatures are quantitative.

Figure 1b shows the calorimetric result obtained by properly calibrating and correcting Fig. 1a. The apparent heat capacity, $C_p^{\#}$, is plotted as a function of the sample temperature, T. Since the heat capacity is defined as "heat brought to a system to increase its temperature, divided by

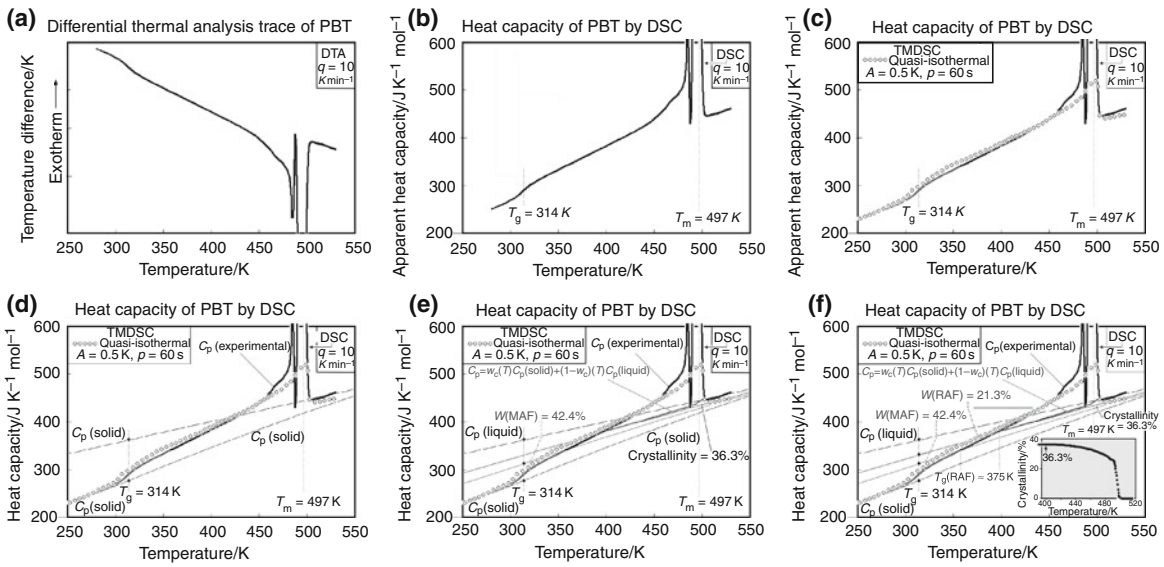

Fig. 1 The stages of development of the thermal analysis of poly(butylene terephthalate), PBT. **a** DTA, **b** conversion to heat capacity (DSC data), **c** addition of quasi-isothermal TMDSC, **d** addition of Data Bank information, **e** evaluation of the RAF, and **f** final PBT analysis

that temperature increase" [1], there is no ambiguity about the direction of the ordinate, and the exothermic and endothermic directions need not to be labeled. To describe the overall change in enthalpy, H, the heat brought into a system, one may start with the basic differential equation:

$$dH = (\partial H/\partial T)_{p,n} dT + (\partial H/\partial n)_{p,T} dn, \quad (1)$$

where the first partial differential, $(\partial H/\partial T)_{p,n}$, represents the thermodynamic heat capacity, C_p, at constant pressure, p, and composition, n. The second partial differential, $(\partial H/\partial n)_{p,T}$ does not affect the temperature. It represents the heat exchanged in a process at constant pressure, p, and temperature, T, called its latent heat, L. The equation applies without restrictions as long as the sample remains in equilibrium over the ranges of T and n investigated and is able to follow the scanning kinetics. Many analyzed systems, however, show a slow response in dH in the glass transition region and during changes in composition, n. The latter are, for example, encountered during chemical reactions or physical changes during order/disorder transitions. Both of these processes are marked in Fig. 1b. In the first case, a time-dependent heat capacity must be introduced in Eq. 1, in the second, a time-dependent latent heat. To still get some useful thermal information, the calorimetry can be carried out either sufficiently slowly so that all changes in H go to completion within the time scale of measurement, or sufficiently fast, so that the system stays metastable during the measurement. Measurement done at comparable time scale of the chemical or physical processes must consider the relevant kinetics.

The kinetics of slow processes can be eliminated by temperature-modulated DSC, TMDSC, in the quasi-isothermal mode of operation where a small modulation, typically 0.05–5.0 K about a constant base temperature, is used for the measurement [7]. Such measurements are limited only by the long-time stability of the calorimeter, and 100 h measurements should be possible. To bypass faster processes, substantial progress has been made in recent years through the developments in fast scanning calorimetry, FSC, using chip calorimetry. Heating and cooling rates as fast as 10^6 K s^{-1} have been demonstrated [8]. Between the two techniques, 10 orders of magnitude of time can be covered by calorimetric experimentation. In case equilibrium cannot be awaited or changes of unstable systems are not outrun, the effect of time is to be included in one or both terms of Eq. 1.

Outside the glass transition ranges, the molecular motion governing the thermodynamics has typical time constants of less than picoseconds and reaches equilibrium quickly relative to the calorimeter response and can then be considered time independent. Any lag due to the kinetics of the latent heat can be dealt with by analyzing the time-dependence of the second term in Eq. 1. The lag due to thermal conductivity arising from sample and calorimeter must, naturally, first be corrected for. Then, the measured, apparent $C_p^{\#}$ is represented by the following two equations:

$$C_p^{\#} = dH/dT = (\partial H/\partial T)_{p,n} + (\partial H/\partial n)_{p,T} \times dn/dT \quad (2)$$

For a given time interval, the change in composition with temperature, dn/dT, may not complete its path from the initial equilibrium state to the final equilibrium. In this case, one must consider the temperature-dependent kinetics, which can be written as:

$$dn/dT = (dn/dt)/(dT/dt) \quad (3)$$

The temperature-dependent kinetics of the system, dn/dt, and, the heating rate, q (=dT/dt), naturally must be evaluated separately. When q is designed to be constant, as in the DTA and standard DSC traces in Fig. 1, dn/dT can be evaluated from curves such as the insets in Fig. 1f and 7, below.

However, first, one has to continue the interpretation of the thermal analysis beyond Fig. 1b. This involves the separation of reversible and irreversible parts by measurement with TMDSC and resolving Eq. 2 [2]. In Fig. 1c, quasi-isothermal TMDSC on the same PBT (cooled at 10 K min^{-1} from the melt) is added. For each marked temperature, TMDSC with an amplitude, A, of ±0.5 K and a period, p, of 60 s was carried out for 20 min. Differences are observed in the glass transition region and the range of changes in order. If needed, the TMDSC experiments can be extended over larger times [7, 9, 10].

The thermodynamic description must be added to a careful characterization the molecules and phases measured not only by chemical structure molar mass, etc., but also by stating their molecular class (small molecules, rigid, or flexible macromolecules [11]) and their phase [9], molecular motion [2], and phase size [12]. It was found that there are 57 possible condensed phases and two types of transitions (glass and order/disorder transitions) necessary for the description [9]. The transitions mark the changes from solid to mobile phase (by the glass transition range, centered at the temperature T_g), and the changes in degree of order (order/disorder transitions, detected by the latent heats at the following temperatures T_o, T_c, for ordering or crystallization, respectively, and T_d, T_i, and T_m for disordering, isotropization, or melting, respectively). These two ranges are marked in Fig. 1b by knowing their typical appearances in a DSC trace. The glass transition is characterized by its change in heat capacity, ΔC_p. At half of this increase in C_p, the value of T_g is chosen. The analysis of the glass transition can be done by changing the modulation parameters [10], as has been documented in detail in for poly(ethylene terephthalate), PET, and polystyrene [2, 13–16]. The disordering in Fig. 1b is connected with an endothermic latent heat at T_m (interrupted by a sharp

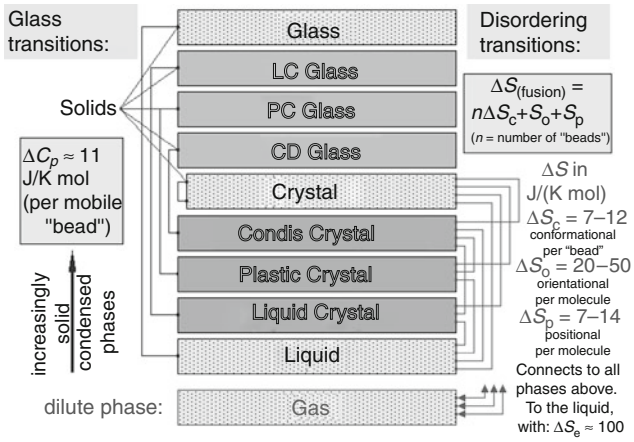

Fig. 2 A schematic of the 10 phases of matter, characterized by their structure, molecular mobility, solidity, and thermal transitions

exotherm—compare also to Fig. 7, below, where an exotherm is seen at much lower temperature without overlap with the endotherm). The initial melting seems to start already between 350 and 450 K. The initial melting is then interrupted by a recrystallization exotherm before complete liquefaction.

A schematic that has been developed over the years to clarify the phases by their macroscopic appearance, properties, molecular order, and molecular motion is displayed in Fig. 2, together with the characteristic thermodynamic parameters of the two transitions, as discussed in Ref. [17].

The three possible size ranges of phases in which their properties change are summarized in Fig. 3 [9, 12]. Before continuing the description of the thermal analysis of PBT, the phase and phase size assignments must be quantified based on the results in Fig. 1c.

To continue the discussion with Fig. 1d, the solid and liquid must be described by their structure *and* molecular motion, as mirrored in the changing thermodynamic functions. In the five solid states of Fig. 2 with different degrees of order, the main molecular motion consists of vibrations. A typical vibrational spectrum was first

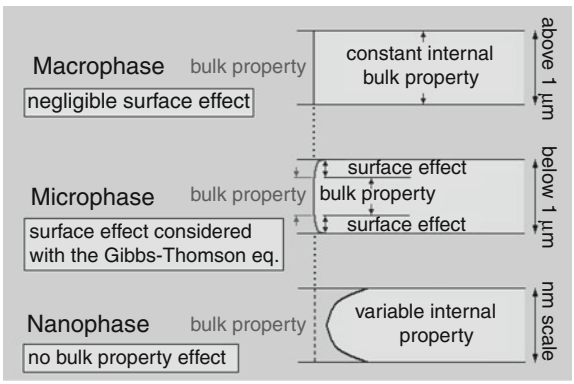

Fig. 3 A schematic of the changes of property with size

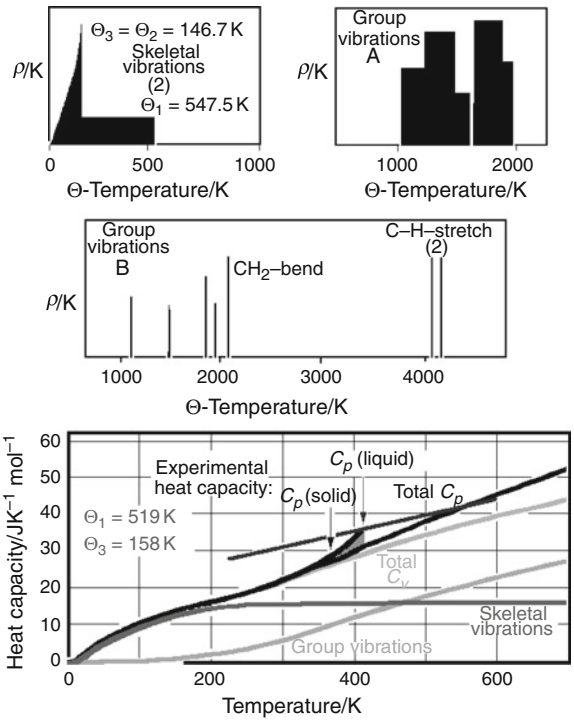

Fig. 4 The connection of the heat capacity to molecular motion in polyethylene

established for crystalline polyethylene, PE [18]. An approximate spectrum which agrees from 0 K to room temperature with the measured C_p is reproduced in Fig. 4 [19]. The connection between Θ-temperatures and frequency, ν, is given by:

$$\Theta = h\nu/k \tag{4}$$

where h is the Planck's constant, and k is the Boltzmann's constant (i.e., 1 K corresponds to 2.08×10^{10} Hz). The frequencies expressed in Θ are useful for thermodynamic considerations. The heat capacity at constant volume, C_v, for the given frequency has reached ≈90% of its excitation-value at the Θ-temperature (for full excitation, $C_v = 8.314$ J K^{-1} mol^{-1}, see also [2, Sect. 2.3]).

The vibrations of the CH_2-group have nine degrees of freedom, of which two are characteristic skeletal vibrations, approximated by the Tarasov functions [20]. The density of states, ρ(K), is plotted in the top left graph of Fig. 4. The three-dimensional and one-dimensional limiting frequencies Θ_3 and Θ_1 fix the C_v (skeletal) as indicated in the bottom plot. For glassy (g) and crystalline (c) PE the C_vs are similar. The crystal and glass have the same Θ_1 value, i.e., both reach full excitation at the same temperature, but Θ_3 for the glass is only ≈80 K. Up to about 50 K the glassy C_v ($\approx C_p$) is slightly larger, but in this temperature range C_p is rather small, so that the change of H_g is only little different from that of the crystal, H_c, as shown in

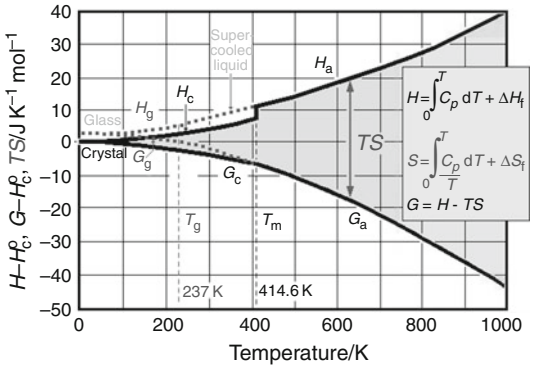

Fig. 5 The three integral thermal functions H, S, and G as derived from C_p for polyethylene

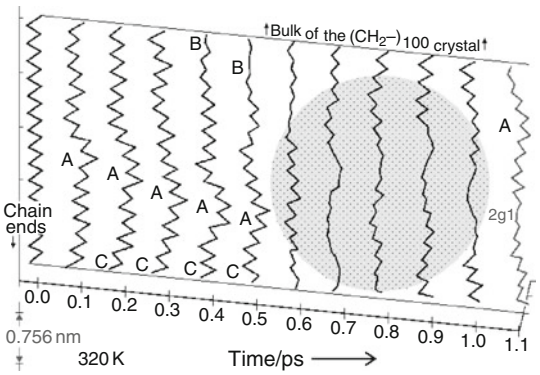

Fig. 6 Molecular dynamics simulation of skeletal vibrations and large-amplitude motion modeled for polyethylene

Fig. 5. The other integral thermodynamic functions derivable from C_p, S and G, are also shown in Fig. 5.

The remaining seven group vibrations for PE are of higher frequency and get excited above 100 K, as seen in the bottom of Fig. 4. The ρ(K) of three of the seven modes of highest frequency (CH-stretch and CH_2-bend) are sufficiently narrow to be represented by single-frequency Einstein functions, while the four others (C–C stretching and CH_2 rocking, twisting, and wagging) are approximated by combinations of averaged frequency regions (upper right graph) and single frequencies (center graph). The sum of the contributions of the group and skeletal vibration, the total C_p (after conversion from C_v), is drawn in the bottom diagram. It represents the vibrational heat capacity of the solid. In Fig. 1d, a similar computation for solid PBT is fitted to the experimental C_p at low temperatures [21].

Also drawn in Fig. 1d is the experimental C_p of liquid PBT. In the temperature range of the melt, above T_m^o, equilibrium is reached for the overall system and both DSC and TMDSC reach the same value. Comparing the C_ps of many different flexible macromolecules in the ATHAS Data Bank [22], one notes that the contributions of the various chemical groups in the backbone and side chain are additive in their C_p contribution. Extensive listings of these contributions have been published for comparison with the experimental data [2, 22–24]. Attempts to assess the details of the vibrational motion in the liquid state were only partially successful [25, 26].

With the baselines of the liquid and solid state C_p established, a quantitative description of the semicrystalline system is attempted with Fig. 1e. From the knowledge that the glass transition is caused by an increasing amount of large amplitude, conformational motions, the time scale of the latter needed to be understood. Figure 6 illustrates a molecular dynamics simulation by supercomputer of a larger section of a polyethylene-like crystal, restricted to the low-frequency skeletal and large-amplitude motion [27]. The letters A, B, and C mark the basic transverse, torsional, and longitudinal vibrations as they form after a random amount of kinetic energy was distributed to reach a temperature of 320 K. The motion starting with the planar, resting CH_2-backbone atoms at time zero in their low-energy, planar zig-zag conformation can be followed. Quite clearly, the example illustrates a phonon collision between 0.5 and 1.0 picoseconds. As a result of this collision, a defect, consisting of two gauche-conformations separated by a trans-conformation (a 2g1 defect), was formed, undergoing a large-amplitude motion. The chain is shortened and twisted by 180°. Typical lifetimes of such defects at 320 K are 1–5 picoseconds (10^{-12} s). A similar large-amplitude motion is expected to be at the root of the cooperative motion in the glass, causing the glass transition [2]. The approximately equal increases of C_p by $\approx$11 J K^{-1} mol^{-1} at the glass transition when describing the chain by its likely mobile beads, as listed in Fig. 2, support this picture. In the discussed examples, a CH_2-group is the bead for PE and the seven beads of PBT consist of one C=O–C_6H_4–C=O-group, four CH_2-groups, and two O-groups) [22].

The surprising result of the quantitative analysis making use of the solid and liquid baselines and the known ΔC_p at T_g and the latent heat in the melting range leads in Fig. 1e to a mobile amorphous fraction, MAF, of 42.4% and a crystallinity, w_c, of 36.3%. The discrepancy of 21.3% can neither be MAF nor crystal. This part of a semicrystalline polymer was earlier identified as a rigid-amorphous fraction, RAF [28]. The discussion of Fig. 3 suggests that this layer of noncrystalline PBT without a bulk-amorphous T_g or latent heat, must be a different *nanophase* reaching its metastability by being coupled to the crystal surface. The same RAF must also be the cause of the cessation of crystallization of flexible, linear macromolecules before reaching equilibrium [17].

Figure 1f, finally, indicates how all stages of the discussion of PBT can be fitted together. In the chosen PBT example, the range of the glass transition of the MAF,

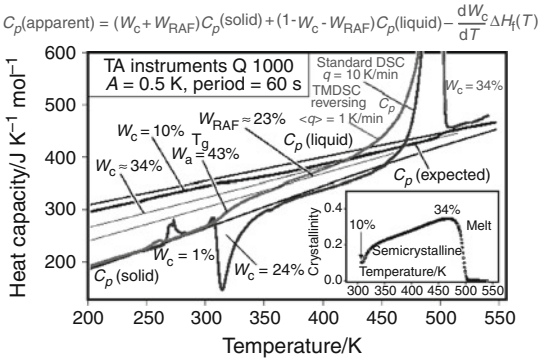

Fig. 7 Thermal analysis of a quenched PBT sample

the RAF, and the melting range do not overlap significantly, so that the change in crystallinity, of importance to fix the mechanical properties of the sample in conjunction with the RAF, can be evaluated over the whole temperature range, as is shown in the inset. Once the temperature range of the RAF glass transition is established, poorer crystallized samples can be analyzed as well [5]. Figure 7 is an example of a partially quenched PBT which shows during heating a major amount of cold crystallization [29]. The sample was analyzed with standard DSC at 10 K min^{-1} as for the slowly cooled sample of Fig. 1, and then analyzed further with TMDSC at 1 K min^{-1} which moves most of the irreversible cold crystallization to the lowest possible temperatures. The expected baseline was calculated with the equation listed in Fig. 7 with the assumption that the glass transition of the RAF goes parallel to the analysis in Fig. 1. The inset shows the cold crystallization and the melting range with its superimposed reorganization and recrystallization. In addition, as in Fig. 1d, locally reversible melting, can be seen [30]. Details about the intermediate structures can be analyzed, as mentioned above, by either extending the time scale of the quasi-isothermal TMDSC to await final equilibrium, or by FSC to move the metable states without significant changes through the unstable temperature ranges of reorganization and recrystallization for identification of their T_g and T_m [31].

Conclusions

The methodology to evaluate the thermal analysis of a semicrystalline, flexible, linear macromolecule was discussed on hand of the example of PBT with Fig. 1a–f and 7, which were analyzed earlier in [5, 21, 27]. Some basic definitions and approaches are shown to be lacking common acceptance, limiting the quantitative interpretations that have been developed over the last 60 years [3]. Just as in other areas of macromolecular science and science in general, the back-integration of progress in specialized areas is lacking and hinders the advance of the basic goal, to establish for a given material the connection of the application properties with synthesis, structure, molecular motion, and thermal and mechanical history. Although the given examples were developed for synthetic macromolecules, it could be shown that the macromolecules of biological origin behave analogously, as is summarized in another symposium of this meeting.

References

1. McNaught AD, Wilkinson A. IUPAC compendium of chemical terminology (the "Gold Book"). Oxford: Blackwell, Scientific; 1997. XML on-line corrected version: http://goldbook.iupac.org 2006, created by Nic M, Jirat J, Kosata B, updates compiled by Jenkins A; ISBN 0-9678550-9-8. doi:10.1351/goldbook.
2. Wunderlich B. Thermal analysis of polymeric materials. Berlin: Springer; 2005. ISBN 978-3-540-23629-0 (Print) 978-3-540-26360-9 (Online).
3. Wunderlich B. A science career against all odds. Berlin: Springer; 2010. ISBN 978-3-642-11195-2 (pp. 9-85–9-86).
4. Barke H-D, Hazari A, Yitbarek S. Misconceptions in chemistry: addressing perceptions in chemical education. Berlin: Springer; 2009. ISBN 978-3-540-70898-3.
5. Pyda M, Nowak-Pyda E, Heeg J, Huth H, Minakov AA, Di Lorenzo ML, Schick C, Wunderlich B. Melting and crystallization of poly(butylene terephthalate) by temperature-modulated and superfast calorimetry. J Polym Sci B. 2006;44:1364–77.
6. Merriam Webster's Collegiate Dictionary, 11th ed. Springfield: Merriam-Webster Inc; 2003. http://www.mw.com/.
7. Boller A, Jin Y, Wunderlich B. Heat capacity measurement by modulated DSC at constant temperature. J Therm Anal. 1994;42:307–30.
8. Minakov AA, Schick C. Ultrafast thermal processing and nanocalorimetry at heating and cooling rates up to 1 Mk/s. Rev Sci Inst. 2007;78:073902-1-10.
9. Wunderlich B. Thermodynamic description of condensed phases. J Therm Anal Calorim. 2010;102:413–24.
10. Boller A, Schick C, Wunderlich B. Modulated differential scanning calorimetry in the glass transition region. Thermochim Acta. 1995;266:97–111.
11. Wunderlich B. A classification of molecules and transitions as recognized by thermal analysis. Thermochim Acta. 1999;340(/341):37–52.
12. Chen W, Wunderlich B. Nanophase separation of small and large molecules. Macromol Chem Phys. 1999;200:283–311.
13. Wunderlich B, Boller A, Okazaki I, Kreitmeier S. Modulated differential scanning calorimetry in the glass transition region, part II. The mathematical treatment of the kinetics of the glass transition. J Therm Anal. 1996;47:1013–26.
14. Boller A, Okazaki I, Wunderlich B. Modulated differential scanning calorimetry in the glass transition region, part III. Evaluation of polystyrene and poly(ethylene terephthalate). Thermochim Acta. 1996;284:1–19.
15. Okazaki I, Wunderlich B. Modulated differential scanning calorimetry in the glass transition region, part V. Activation energies and relaxation times of poly(ethylene terephthalate)s. J Polym Sci B. 1996;34:2941–52.
16. Okazaki I, Wunderlich B. Modulated differential scanning calorimetry in the glass transition region, part VI. Model calculations based on poly(ethylene terephthalate). J Therm Anal. 1997;49:57–70.

17. Wunderlich B. Quasi-isothermal temperature-modulated differential scanning calorimetry (TMDSC) for the separation of reversible and irreversible thermodynamic changes in glass transition and melting ranges of flexible macromolecules. Pure Appl Chem. 2009;81:1931–52.
18. Wunderlich B. Motion in polyethylene II. Vibrations in crystalline polyethylene. J Chem Phys. 1962;37:1207–16.
19. Pyda M, Bartkowiak M, Wunderlich B. Computation of heat capacities of solids using a general Tarasov equation. J Therm Anal Calorim. 1998;52:631–56.
20. Wunderlich B, Baur H. Heat capacities of linear high polymers. Fortschr Hochpolymeren Forsch (Adv Polymer Sci). 1970;7:151–368.
21. Pyda M, Nowak-Pyda E, Mays J, Wunderlich B. Heat capacity of poly(butylene terephthalate). J Polym Sci B. 2004;42:4401–11.
22. Wunderlich B. The Athas Data Base on heat capacities of polymers. Pure Appl Chem. 1995;67:1019–1026. For data via the internet, see http://athas.prz.rzeszow.pl.
23. Gaur U, Cao M-Y, Pan R, Wunderlich B. An addition scheme of heat capacities of linear macromolecules. Carbon backbone polymers. J Therm Anal. 1986;31:421–45.
24. Pan R, Cao M-Y, Wunderlich B. An addition scheme of heat capacities of linear macromolecules. Part II, backbone-chains that contain other than C-bonds. J Therm Anal. 1986;31:1319–42.
25. Loufakis K, Wunderlich B. Computation of heat capacity of liquid macromolecules based on a statistical mechanical approximation. J Phys Chem. 1988;92:4205–9.
26. Pyda M, Wunderlich B. Computation of heat capacities of liquid polymers. Macromolecules. 1999;32:2044–50.
27. Sumpter BG, Noid DW, Liang GL, Wunderlich B. Atomistic dynamics of macromolecular crystals. Adv Polymer Sci. 1994;116:27–72.
28. Cheng SZD, Pan R, Wunderlich B. Thermal analysis of poly(butylene terephthalate), its heat capacity, rigid-amorphous fraction and transition behavior. Makromol Chem. 1988;189:2443–58.
29. Wunderlich B. Theory of cold crystallization of high polymers. J Chem Phys. 1958;29:1395–404.
30. Wunderlich B. Reversible crystallization and the rigid-amorphous phase in semicrystalline macromolecules. Progr Polym Sci. 2003;28(3):383–450.
31. Wunderlich B. The influence of liquid to solid transitions on the changes of macromolecular phases from disorder to order. Thermochim Acta. 2010. doi:10.1016/j.tca.2010.09.005; in print.